Research Article

For reprint orders, please contact: reprints@futuremedicine.com

Biomarkers in Medicine

Study and detection of potential markers for predicting metastasis into lymph nodes in prostate cancer

Ioannis Papasotiriou*[,1], Panagiotis Apostolou[2], Dimitrios-Athanasios Ntanovasilis[2], Panagiotis Parsonidis[2], Daniar Osmonov[3] & Klaus-Peter Jünemann[3]

[1]Research Genetic Cancer Centre International GmbH, Zug 6300, Switzerland

[2]Research Genetic Cancer Centre S.A., Florina 53100, Greece

[3]Department of Urology & Pediatric Urology, University Medical Center Schleswig-Holstein, Kiel 24105, Germany

*Author for correspondence: Tel.: +41 041 725 0560; papasotiriou.ioannis@rgcc-international.com

Hormone-refractory prostate carcinoma has a different cell surface protein profile than hormone-sensitive prostate carcinoma, which provides migration ability and interactions with organs/tissues. Detection and association of these proteins with lymph node metastasis via lymphadenectomy might be beneficial for patients. Gene expression analysis in hormone-refractory and hormone-sensitive commercial cancer cell lines was performed and, after co-cultivation with osteoblasts or endothelial cells, knockdown experiments followed to validate potential biomarkers. "*Myeloid-associated differentiation markers, myosin 1b and phosphatidylinositol-4-phosphate-5-kinase type 1 alpha are implicated in metastasis,*" their knockdown altered the expression of key regulators of endothelial-mesenchymal transition, invasion, motility and migration. In primary prostate tumors, these genes could be an indicator for future metastasis into lymph nodes.

First draft submitted: 24 June 2020; Accepted for publication: 24 July 2020; Published online: 17 August 2020

Keywords: bone metastasis • lymph node metastasis • MYADM • MYO1B • PIP5K1A • prostate cancer

Prostate cancer is the most common cancer type among men worldwide. Treatment management depends on whether the carcinoma is hormone refractory or hormone sensitive. Hormone-refractory prostate carcinoma has different surface proteins, which provide different migration ability and interactions with organs and tissues. By contrast, hormone-sensitive prostate carcinoma migrates and often metastasizes. Therefore, the authors analyzed prostate carcinoma cell lines grown in a model environment resembling a bone or lymph node environment to detect biomarkers that can distinguish if metastasis will occur through bone or lymph nodes. The use of 3D cell cultures instead of 2D simulated the tumor microenvironment much better. Matrigel (Corning, Kaiserslautern, Germany) is a cell culture component that can provide growth factors, hormones and other molecules that reflect physiologically relevant conditions of *in vivo* cell interactions [1]. During tumor progression, cancer cells interact with the microenvironment and promote immune tolerance and angiogenesis. This interaction also promotes tumor survival, proliferation and metastasis. It has already been demonstrated that endothelial cell interaction with lung cancer cells changes cancer cell morphology to a mesenchymal-like state, decreases apoptosis rate, increases migration and enhances tube formation rate. Compared with traditional wound healing assays, endothelial tube formation in Matrigel is more similar to the physiological conditions underlying angiogenesis and vessel formation [2]. The authors used a 3D cell culture model with extracellular matrix, engineered tissue osteoblasts using cell sheet techniques and seeded prostate cancer cell lines in this co-cultivation system. The aim of the authors' study was to identify potential markers that are already known to exist in prostate cancer but whose expression alters upon metastasis to lymph nodes in a different way than that seen in bone metastasis. Lymph nodes can be similarly developed on a co-cultivation model using endothelial cells and prostate cancer cells. The authors depleted or inhibited relevant cancer cell markers or membrane proteins to determine which proteins are involved in colonization and metastasis. Overexpressed cancer cell genes were knocked down using RNAi techniques to validate the authors' *in vitro* cell

Future Medicine

culture model and to investigate metastatic processes and the role of these genes during cellular interactions. The authors' results reveal the specific genes that are essential for lymph node metastasis and that represent potential biomarkers for informing lymph node resection therapy.

Methods

Cell lines

All cell lines were obtained commercially. The authors selected two human prostate carcinoma cell types. One group of cell lines was hormone sensitive, and the other was hormone refractory. The hormone-sensitive group consisted of three cell lines: LNCap clone FGC (89110211; European Collection of Authenticated Cell Cultures [ECACC], Salisbury, UK), VCaP (06020201; ECACC) and MDA-PCa 2b (CRL-2422™; American-Type Culture Collection, Wesel, Germany). The hormone-refractory group also consisted of three cell lines: PC3 (90112714; ECACC), DU 145 (HTB-81; American-Type Culture Collection) and SerBob (10021101; ECACC). All cell lines were cultured according to manufacturer instructions with the appropriate medium and supplements at 37°C in 5% CO2. The cancer cell lines were grown in a model environment resembling a bone or lymph node environment. The bone-like environment was developed using a co-cultivation model of human osteoblasts (C-12720; PromoCell, Heidelberg, Germany) and each prostate cancer cell line. Lymph node-like environments were similarly developed using a co-cultivation model of the endothelial cell line, primary human dermal lymphatic endothelial cells (C-12216; PromoCell) and each prostate cancer cell line. In addition, 3D cell cultures were grown with Matrigel (354262). Cancer cells were mixed with endothelial cells. Mixed cells were resuspended in 1:1 Matrigel-RPMI and plated in the well centers in 24-well plates. Culture plates were incubated at 37°C for 30 min to let the Matrigel solidify. Cells were co-cultured for 4 days before analysis. The Matrigel co-culture was broken down by incubating the plates at 4°C for 1 h, which allowed the Matrigel to liquify while having little effect on cell viability. Then, the 3D culture was dissolved into the medium by gently pipetting each well several times. The medium was removed, and the wells were washed with ice-cold phosphate-buffered saline (PBS) to ensure minimal cell loss. The authentication of cell lines was performed using short tandem repeat tests, and all cell lines were tested for *Mycoplasma*.

Flow cytometry

All cell lines were initially tested for prostate-specific membrane antigen (PSMA) using mouse anti-human PSMA antibody conjugated with phycoerythrin (AB77228; Abcam, Cambridge, UK). Cells were trypsinized, washed in PBS and 2% bovine serum albumin and stained using the antibody concentration suggested by the manufacturer. Cells were incubated for 20 min and then washed with PBS and 2% bovine serum albumin. Next, cells were centrifuged for 5 min at 1600 rpm and resuspended in 500 µl PBS. Data acquisition was performed using a BD FACSCalibur flow cytometer equipped with two lasers (blue and red). Data were analyzed using FCS Express 6. Gates were drawn using unstained samples on FL2 and SS dot plots for PSMA expression.

DNA microarrays

Total RNA from cultured cells was extracted using an RNeasy mini kit (74105; Qiagen, Hilden, Germany). Next, 1 µg extracted RNA was prepared for DNA microarray experiments using an Amino Allyl MessageAmp II kit (AM1753; Ambion, Berlin, Germany). Labeling was performed with an Amersham CyDye post-labeling reactive dye pack (RPN5661; GE Healthcare, Freiburg im Breisgau, Germany). Reference (Cy3-labeled) and prostate samples (Cy5-labeled) were mixed together and co-hybridized using the Human MI ReadyArray platform (HS1100; Microarrays Inc., AL, USA). An HS 400 Pro hybridization station (Tecan) was used for pre- and post-hybridization processes and washing–drying steps. Slides were imaged on an InnoScan 710 (Innopsys) scanner with 5-µm resolution. Scanned microarray image data were processed using Array-Pro Analyzer 6.3 software. Data were normalized using background subtraction.

Gene expression analysis

Total RNA samples (1 µg) were used for cDNA synthesis and real-time quantitative PCR (RT-qPCR) reactions. For cDNA synthesis, the authors used the PrimeScript RT reagent kit (RR037A; Takara, Saint-Germain-en-Laye, France) and for RT-qPCR the KAPA SYBR Fast master mix universal (×2) (KK4618; Kapa Biosystems, Hamburg, Germany); the final reaction was 20 µl. All the primers for genes of interest and housekeeping genes were designed on Beacon Designer 8. Primer sequences were evaluated using Basic Local Alignment Search Tool (https://blast.ncbi.nlm.nih.gov/Blast.cgi) searches to exclude primers that would amplify undesired genes

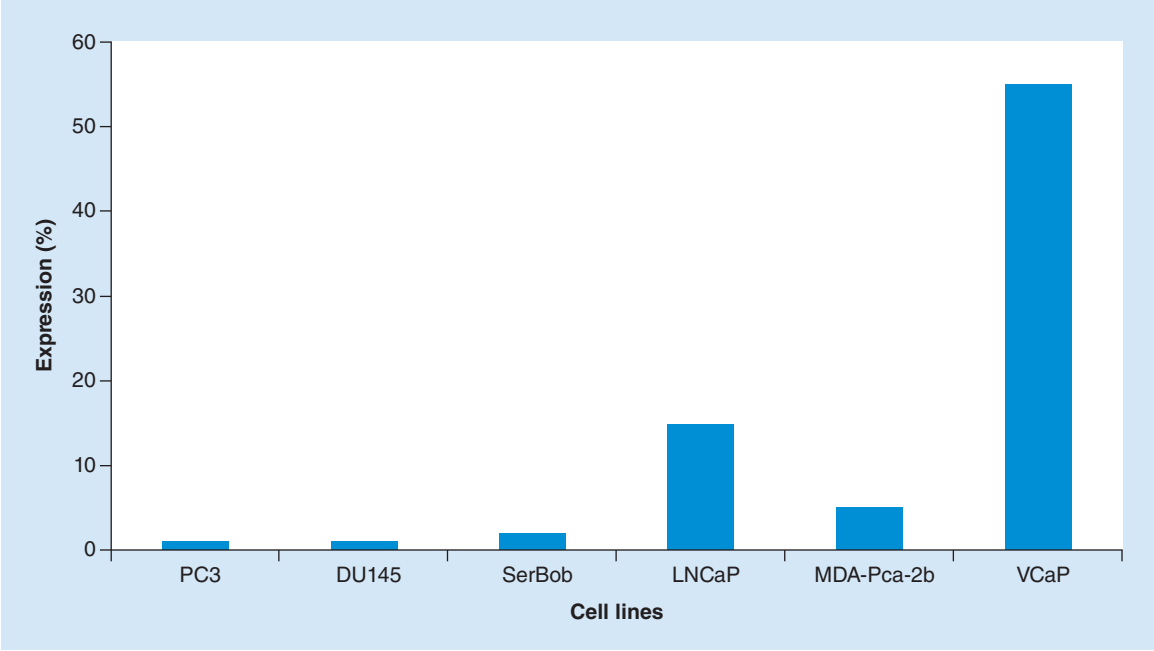

Figure 1. PSMA expression in prostate cancer cell lines.
PSMA: Prostate-specific membrane antigen.

(Supplementary Table 1). Samples were analyzed by PCR as follows: 95°C for 2 min, followed by 45 cycles of 95°C for 10 s and 59°C for 30 s. Upon amplification, a melting curve analysis was performed from 70°C to 90°C at 0.5°C increments for 5 s at each step. PCR data were analyzed by the ΔΔCt method.

In all reactions, cDNA synthesized from Universal Human Reference RNA (740000-41; Agilent, CA, USA) was used as a positive control. Additional controls, including no-template and negative controls, were also used in all experiments. The reactions were performed in triplicate.

Knockdown experiments

To create stable knockdown cells, the authors used a BLOCK-iT inducible H1 RNAi entry vector kit (K492000; Thermo Fisher Scientific, Dreieich, Germany). Short hairpin RNA sequences were based on previous siRNA molecules (Supplementary Table 2). Cloning and transfection were performed using competent cells according to manufacturer instructions. The recombinant DNA was isolated and used to transform prostate cancer cell lines using Xfect reagent (631317; Takara). Cells were selected using Zeocin selection reagent (R25001; Thermo Fisher Scientific) and co-cultured with endothelial cells. In positive knockdown cells, genes correlated with metastasis, invasion and endothelial-mesenchymal transition were analyzed by RT-qPCR. The analyzed genes included *CD44*, *CDH1*, *CDH2*, *CTNNB1*, *DPP4*, *ITGA5*, *ITGAV*, *ITGB1*, *ITGB2*, *KRT19*, *SNAI1*, *SNAI2*, *TWIST1*, *CAV2*, *CLDN3*, *EGFR*, *DSC1*, *FN1*, *MET*, *EPCAM* and *VIM*.

Statistical analysis

The statistical analysis included one way analysis of variance (one-way ANOVA) and Tukey's Q post-test. All analyses were performed using PAST statistical software.

Results

Flow cytometry

Hormone-sensitive cell lines (LNCaP, MDA-PCa-2b and VCaP) expressed PSMA at various levels, as expected (Figure 1). By contrast, hormone-refractory cell lines (PC3, DU145 and SerBob) showed much lower PSMA expression [3].

10.2217/bmm-2020-0372

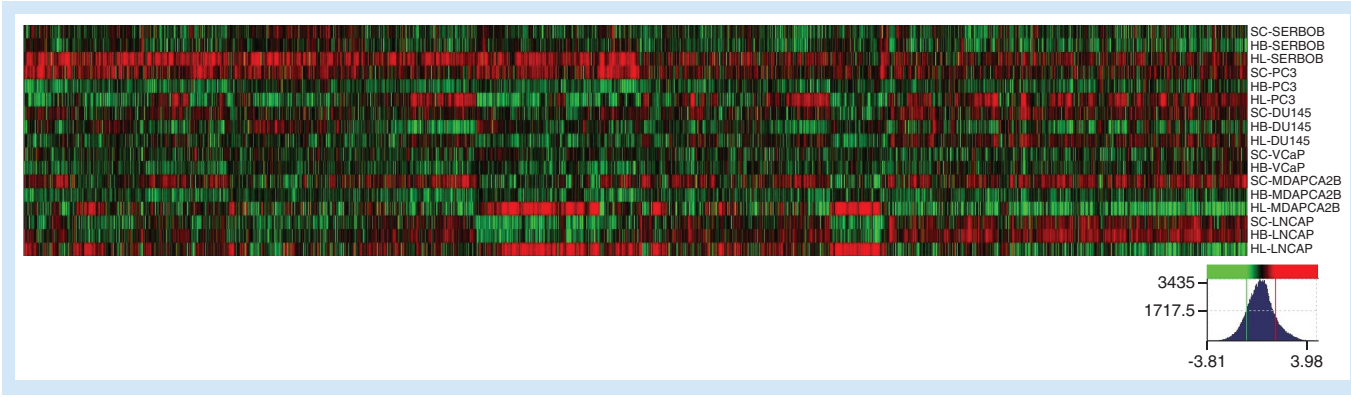

Figure 2. Heatmap of microarray gene expression assays.

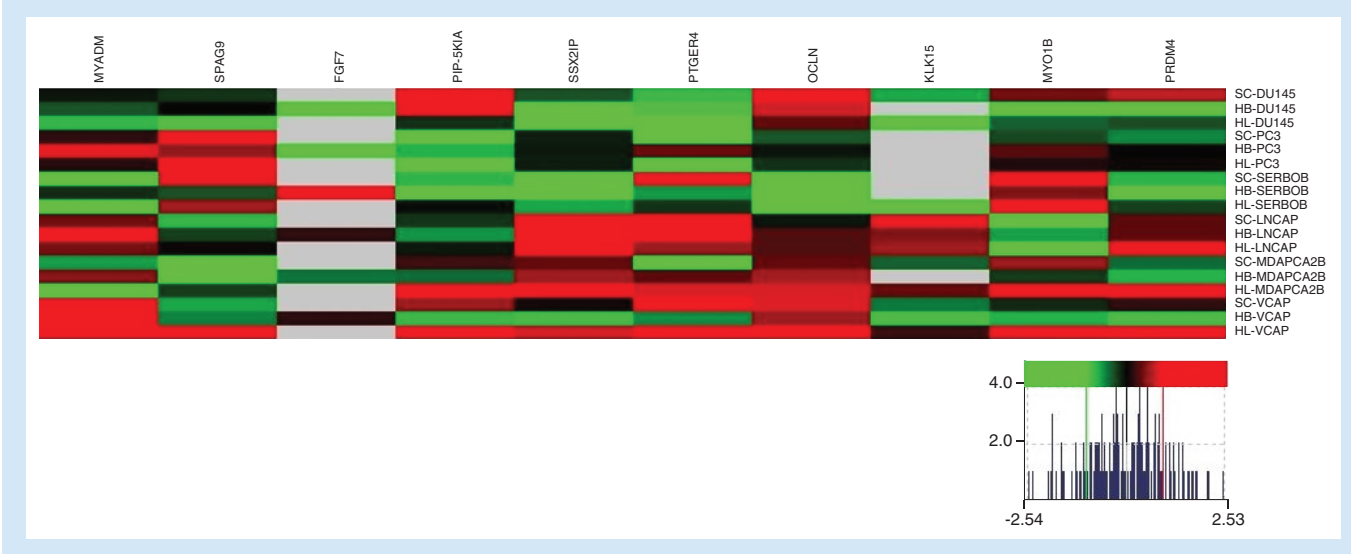

Figure 3. Heatmap of qPCR experiments for selected genes.
qPCR: Quantitative PCR.

Marker validation

Microarray experiments revealed hundreds of differentially expressed genes when co-cultivated with osteoblasts or endothelial cells (Figure 2). The authors also compared gene expression between co-cultivated cells, osteoblasts, endothelial cells and cancer cell lines. Genes highly expressed before co-cultivation were not included in the final analysis.

After validating the differentially expressed genes, *MYADM*, *PIP5K1A*, *PTGER4*, *MYO1B*, *SPAG9*, *OCLN*, *PRDM4*, *SSX2IP*, *KLK15* and *FGF7* were selected for further experiments (Figure 3). These were expressed in the initial cancer cell line (before co-cultivation) and had different expression profiles after culture. The genes that were finally selected were *MYADM*, *PIP5K1A* and *MYO1B* (Figure 4).

Gene knockdown

Permanent knockdown was evaluated after incubation for 4 weeks with the appropriate short hairpin RNA vector (Table 1).

Post-knockdown gene expression

Permanent knockdown was efficient for *MYADM*, *MYO1B* and *PIP5K1A*. Thus, these genes were further analyzed (Figure 5). *MYADM* knockdown caused decreased *ITGB1*, *IGF1R* and *TWIST1* expression in all cell lines.

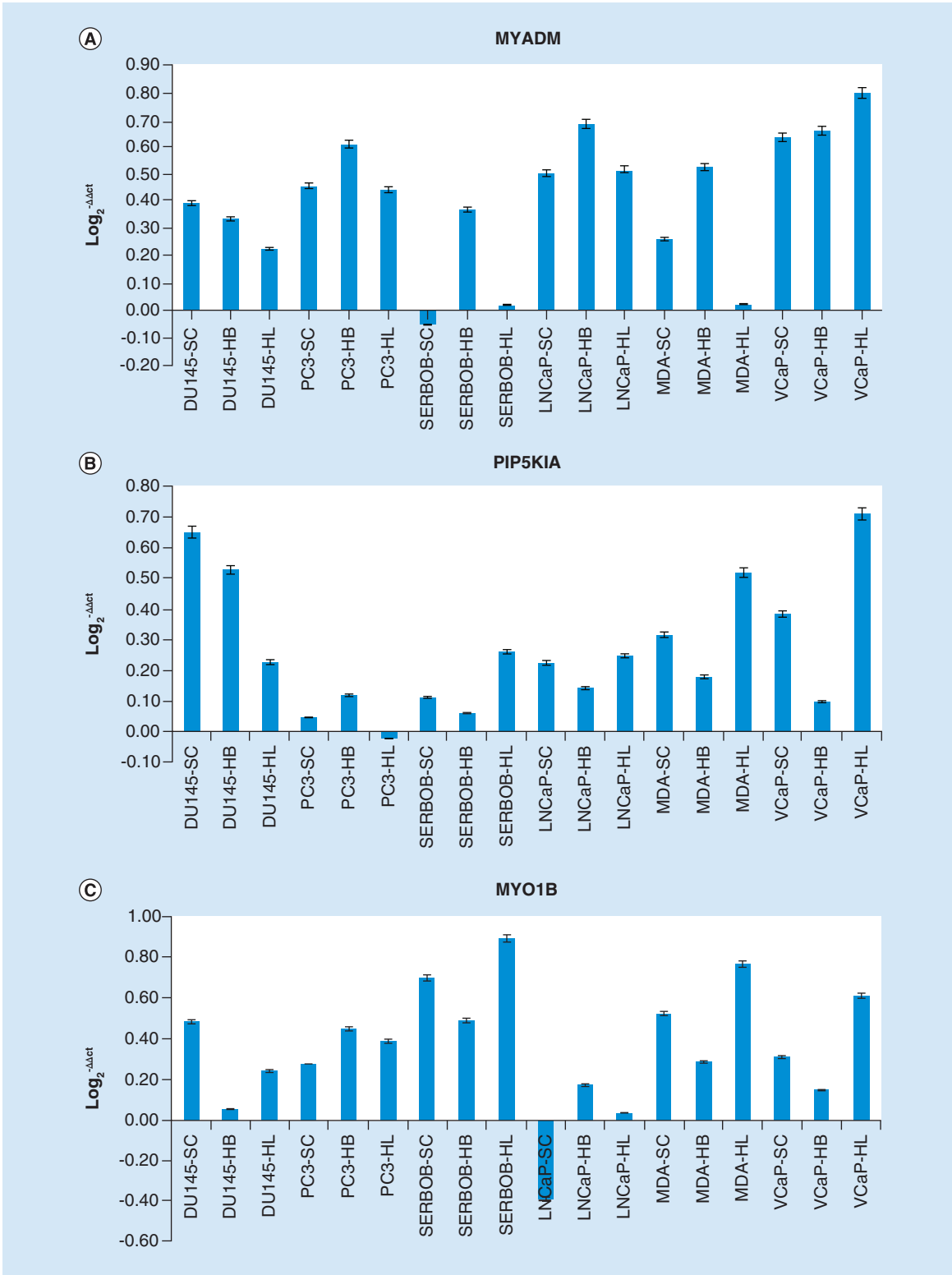

Figure 4. Gene Expression in single-culture and in co-cultivation. (A) *MYADM*; **(B)** *PIP5K1A* and **(C)** *MYO1B* gene expression.
SC: Scaffolds; HB: Co-culture with osteoblasts; HL: Co-culture with endothelial cells.

10.2217/bmm-2020-0372

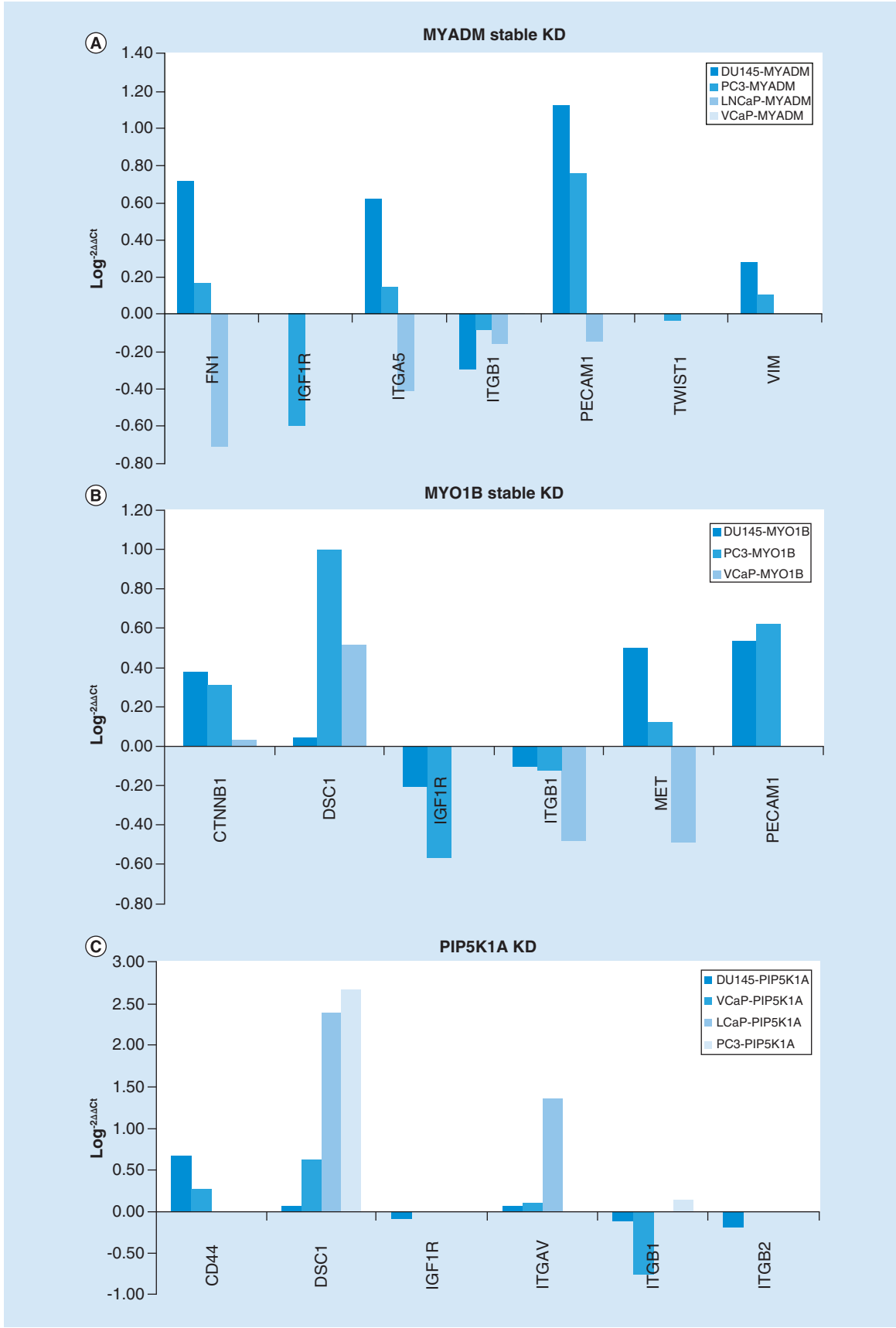

Figure 5. Gene Expression in single-culture and in co-cultivation. Gene expression after **(A)** *MYADM*, **(B)** *MYO1B* and **(C)** PIP5K1A knockdown.

Table 1. Percent knockdown.

Genes	DU145	PC3	VCaP	LNCaP
MYADM	Complete	Complete	Complete	Complete
MYO1B	25.02	85.9	45.52	–
PIP5K1A	20.77	25.49	69.86	40.45

Complete knockdown indicates that the gene was not more expressed post-knockdown (i.e., no successful knockdown).

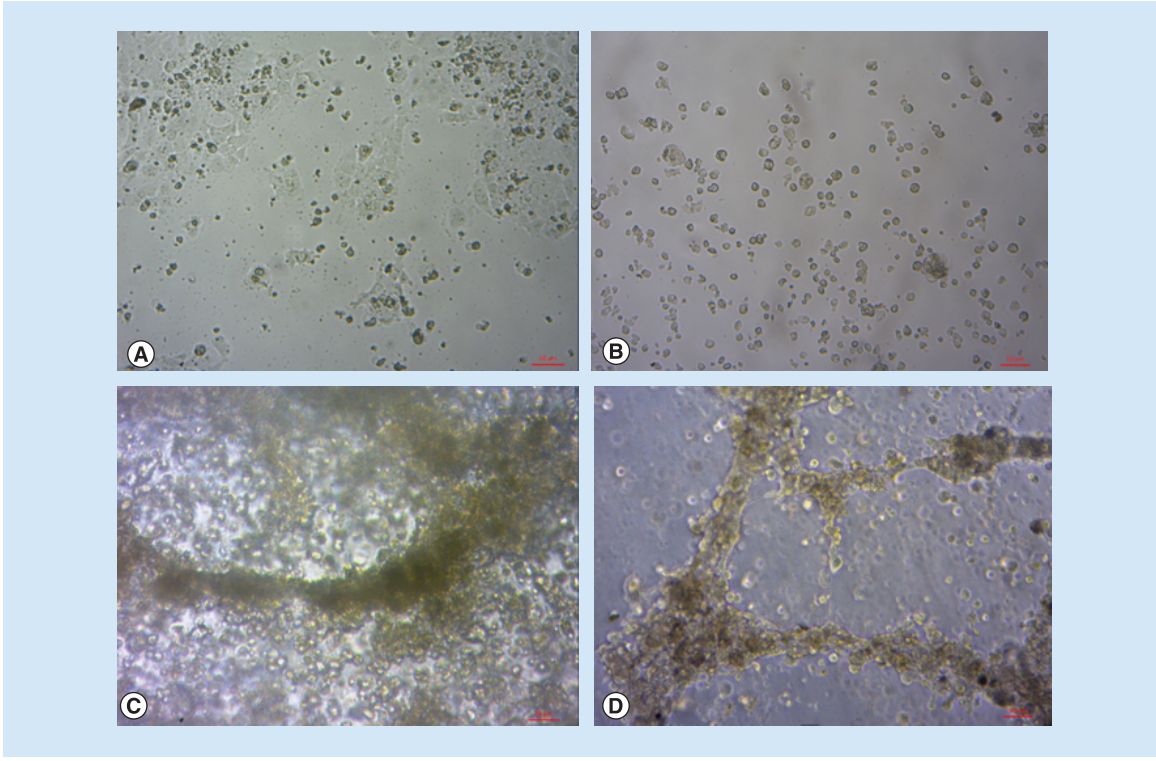

Figure 6. PC3 cell culture pre- and post-knockdown. (A) 2D culture of PC3 cells. **(B)** 2D culture of PC3 cells after *PIP5K1A* knockdown. No matrix formation is observed. **(C)** 3D culture of PC3 cells co-cultured with endothelial cells in Matrigel. Cells grow next to the endothelial cells, forming clusters with them. **(D)** 3D culture of PC3 cells after *PIP5K1A* knockdown and co-culture with endothelial cells in Matrigel. Cells grow as single cells, without making junctions. Cultures were imaged at ×10 magnification.

Further, *FN1*, *ITGA5*, *ITGAV* and *PECAM1* were upregulated in hormone-refractory cell lines but downregulated in hormone-sensitive cells. *MYO1B* knockdown downregulated *ITGB1* and *IGF1R* in all tested cell lines and upregulated *CTNNB1* and *DSC1*. The authors observed *MET* and *PECAM1* overexpression only in hormone-sensitive cell lines. Additionally, *ITGB1* and *IGF1R* were downregulated after *PIP5K1A* knockdown. The authors' results revealed crosstalk between several tested genes, which could explain the expression patterns in some of the associated genes.

The authors also investigated cellular morphology of the previous specific markers pre- and post-knockdown. There were no signs of matrix formation after knockdown (Figure 6B). PC3 cell morphology clearly changed after *PIP5K1A* knockdown (Figure 6B). The authors then co-cultivated cells with endothelial cells in Matrigel. Endothelial tube formation was observed in the co-cultures (Figure 6C & D). PC3 control cells appeared to be able to grow close to the human umbilical vein endothelial cell formations and to form cell clusters (Figure 6C). However, PC3 cells with *PIP5K1A* knockdown appeared to grow as single cells, without making junctions with other cells or human umbilical vein endothelial cell formations (Figure 6D).

10.2217/bmm-2020-0372

Discussion

The identification of a specific molecule expressed in prostate tumors that might be used as an indicator of lymph node metastasis would be greatly beneficial. This marker would be particularly useful for distinguishing metastasis to lymph nodes or osteoblasts when gene expression changes based on differential expression in osteoblasts or endothelial cells. Thus, the authors selected *SPAG9*, *FGF7*, *PIP5K1A*, *MYADM*, *PTGER4*, *OCLN*, *MYO1B*, *PRDM4* and *KLK15*, which are expressed in prostate tumors. Three of these genes, *MYADM*, *MYO1B* and *PIP5K1A*, were selected for further experiments since expression is different between cells co-cultivated with endothelial cells or osteoblasts. These three genes might be associated with metastasis to lymph nodes, and the authors hypothesized that the downregulation of their expression should lead to alteration of gene expression in factors essential in metastasis, such as molecules involved in invasion, motility and adhesion. For cell lines with successful gene knockdown, gene expression analysis of genes associated with invasion, motility, adhesion, metastasis, proliferation and aggressiveness was used to investigate the results.

The lipid kinase *PIP5K1A* phosphorylates PtdIns4P to PtdIns(4,5)P2. In the nucleus, *PIP5K1A* interacts with Star-PAP via PtdIns(4,5)P2, thereby regulating Star-PAP activity and downstream gene expression [4]. Star-PAP polyadenylates a select subset of mRNAs involved in the oxidative stress response, apoptosis and cancer. Importantly, Star-PAP possesses tumor-suppressing activity in breast cancer [5]. In addition to being involved in PtdIns(4,5)P2 production, *PIP5K1A* is an upstream regulator of Rac1, which is involved in the control of actin dynamics and cell migration [6].

PIP5K1A regulates the PI3K/AKT/androgen receptor (AR) pathway and results in cancer cell proliferation, invasion and survival via the production of PtdIns(4,5)P2 [7]. In prostate cancer, overexpression of *PIP5K1A* is related to poor prognosis and is associated with elevated AR levels. Metastatic lesions contain significantly higher *PIP5K1A* and AR levels compared with primary tumors [8]. Increased AR expression leads to the formation of protein complexes that contain the cell cycle protein CDK1 in their nuclei. In addition, the previously mentioned targets have already been established, yet there are no data to date that support their role in lymph node metastasis [9].

MYADM belongs to the myelin and lymphocyte protein family, which is involved in membrane trafficking processes [10]. *MYADM* is involved in the membrane organization required for cell migration through Rac1 co-localization. The role of *MYADM* in metastasis is also supported by new 3D experiments [11]. Rac1 is a Rho family GTPase that regulates cell spreading and actin-mediated lamellipodia extension [12]. *MYADM* also regulates ezrin, radixin and moesin (ERM) proteins, which connect the plasma membrane and cytoskeleton. These proteins regulate the structure and function of filopodia, thereby regulating signaling processes such as motility and cytokinesis [13]. ERM expression in turn regulates intercellular adhesion molecule expression [14,15]. Further, upon ERM activation, N-terminal four-point-one, ezrin, radixin and moesin interact with PtdIns(4,5)P2 [16].

MYO1B is a member of the myosin protein superfamily and is involved in organelle transportation, generation of membrane tension and muscle contraction [17]. Cells with high metastatic potential, including prostate cancer cell lines, highly express *MYO1B*. This protein directly influences actin organization and cell morphology, factors that contribute to metastasis. PC3 cells express higher levels of *MYO1B* than LNCaP cells. Increased endogenous *MYO1B* levels in highly metastatic cells lead to increased cortical tension; therefore, cells are able to move through stiff extracellular matrices *in vivo*. *MYO1B* is associated with migration in prostate cancer, which is also supported by the 3D cultures used in the authors' experiments [18]. *MYO1B* is associated with proliferation, migration and invasion in other cancer types [19,20] and contributes to membrane trafficking by controlling organelle shape [21]. Further, *MYO1B* might be involved in migration by participating in filopodia and lamellipodia formation and regulating actin assembly [22,23]. The localization of *MYO1B* within filopodia requires phosphoinositide binding, indicating additional phosphoinositide roles in migration [24].

The genes studied post knockdown were selected according to specific cancer characteristics, and in particular prostate cancer characteristics. The transmembrane glycoprotein CD44 is associated with cell–cell and cell–matrix adhesion. Abnormal CD44 expression is associated with different cancer types, including prostate carcinoma. Further, CD44 is downregulated in prostate tumors [25]. However, CD44 has a functional role in invasion [26]. *ITGAV* is implicated in prostate cancer progression [27]. Furthermore, *ITGAV* is associated with prostate cancer maintenance and bone metastasis [28]. *Twist1* is a transcription factor that regulates the endothelial-mesenchymal transition and is implicated in prostate cancer metastasis [29]. *VIM* is also involved in prostate cancer invasiveness through Src regulation [30], which affects invasiveness and prostate cancer cell motility [31]. Beta-catenin is correlated with adhesion and signal transduction. Several mutations in beta-catenin are observed in prostate cancer [32], and

overexpression can promote invasive prostate cancer [33]. *DSC1* expression facilitates metastasis, aggressive tumor behavior and poor prognosis in squamous carcinomas [34]. *ITGA5* is a migration-related gene that plays an important role in cell adhesion and migration. The expression of *ITGA5* can increase the formation of mother vessels by stimulating the VEGF-A pathway. *ITGA5* downregulation prevents metastasis. *ITGB1* is involved in cell adhesion and metastasis and is involved in TGFβ signaling in prostate cancer. Together, these proteins contribute to the switch from tumor suppression to oncogenesis [35]. *IGF1R* is also involved in prostate cancer and enhances tumor growth, migration and angiogenesis [36]. Therefore, *MYADM*, *PIP5K1A* and *MYO1B* in primary prostate cancer tumors could indicate future lymph node metastasis and help guide lymph node dissection in prostate cancer patients.

The dissection of lymph nodes is generally based on D'Amico classification risk, which is associated with prostate-specific antigen level, Gleason score and clinical stage [37]. Based on recent experimental data, the value of pelvic lymph node dissection in patients with prostate cancer – based on D'Amico risk – remains unclear [38]. In addition, other classification systems, such as the Candiolo classifier, have been proposed for managing prostate cancer treatment [39]. These systems require the testing of several parameters and so waste valuable time. A simple method that could be performed during surgery and provide evidence of any potential metastasis might be more helpful. Based on the authors' experimental data, which of course must be validated using clinical samples, studying one of the three tumor markers investigated here using, for example, histological techniques may contribute to a rapid classification system independent of hormone sensitivity. In recent years, many diagnostic techniques have been used for lymph node staging in prostate cancer since lymph node dissection is associated with a survival benefit in patients with metastatic prostate cancer undergoing radical prostatectomy [40]. However, the majority of these require specific equipment and knowledge and, most importantly, cannot be performed during the time window of prostate cancer surgery [41]. *MYADM*, *MYO1B* and *PIP5K1A* constitute 3 biomarkers that are detected in primary hormone-refractory and hormone-sensitive prostate tumors. As previously mentioned, it is mainly hormone-refractory prostate cancer that metastasizes to lymph nodes and, subsequently, to other organs and tissues. In these cases, lymph node dissection is preferable and beneficial since it can prevent metastasis from cascading through the lymph nodes. However, not all cases of prostate cancer lead to lymph node metastasis; therefore, lymphadenectomy in such patients could cause additional problems. For this reason, biomarkers that can predict metastasis of the primary tumor to lymph nodes are required. Additionally, the detection of such biomarkers should be performed using fast and simple methods, such as histological techniques, so any decision about dissection can be made immediately, even during surgery. For all these reasons, the biomarkers *MYADM*, *MYO1B* and *PIP5K1A* may be used to classify primary prostate tumors with high metastatic lymph node potential, regardless of whether they are hormone-sensitive or hormone-refractory.

Conclusion

To sum up, biomarkers that may be associated with prostate cancer metastasis to lymph nodes would be helpful for prostate cancer management since the removal of lymph nodes could be beneficial for the patient. The authors identified genes that are expressed in prostate cancer and that have different expressions when co-cultivated with osteoblasts or endothelial cells. These genes are implicated in processes required for metastasis. Knocking down these genes altered the expression of key endothelial-mesenchymal transition regulators, invasion, motility and migration. Therefore, the presence of *MYADM*, *PIP5K1A* or *MYO1B* in primary tumors could indicate future lymph node metastasis. Despite the fact that data in cancer cell lines are encouraging, *MYADM*, *PIP5K1A* and *MYO1B* expression should be studied in prostate cancer cells as well as in lymph node tissues so that these markers may be used for predicting lymph node metastasis from the prostate.

Future perspective

If biomarkers *MYADM*, *PIP5K1A* and *MYO1B* are validated on patient samples, it will enable oncologists and surgeons to determine whether lymphadenectomy might be beneficial for their prostate cancer patients. By using rapid staining tests during surgery, physicians can observe the presence of markers associated with lymph node metastasis and decide whether lymphadenectomy should be performed.

10.2217/bmm-2020-0372

Summary points

- Co-cultures (3D) of prostate cell lines with osteoblasts or endothelial cells simulated the tumor microenvironment.
- *MYADM*, *PIP5K1A* and *MYO1B* were overexpressed in prostate cancer cells.
- *MYADM*, *PIP5K1A* and *MYO1B* were associated with metastasis to lymph nodes.
- Knockdown of *MYADM*, *PIP5K1A* and *MYO1B* led to a decrease in genes essential for invasion, motility and migration.

Author contributions

I Papasotiriou supervised the study and drafted the manuscript. P Apostolou performed molecular biology assays and drafted the manuscript. D-A Ntanovasilis performed flow cytometry assays. P Parsonidis performed cell culturing assays. D Osmonov supervised the study. K-P Jünemann supervised the study. All authors have read and approved the final manuscript.

Financial & competing interests disclosure

The authors have no relevant affiliations or financial involvement with any organization or entity with a financial interest in or financial conflict with the subject matter or materials discussed in the manuscript. This includes employment, consultancies, honoraria, stock ownership or options, expert testimony, grants or patents received or pending, or royalties.

No writing assistance was utilized in the production of this manuscript.

Ethical conduct of research

The authors state that they have obtained appropriate institutional review board approval or have followed the principles outlined in the Declaration of Helsinki for all human or animal experimental investigations. In addition, for investigations involving human subjects, informed consent has been obtained from the participants involved. All procedures were conducted according to the standards of safety, bioethics and validation. The study was reviewed and approved by the bioethical committee of the Research Genetic Cancer Centre Group.

Data sharing statement

The datasets used and/or analyzed during the current study are available from the corresponding author on reasonable request.

References

Papers of special note have been highlighted as: • of interest; •• of considerable interest

1. Fang Y, Eglen RM. Three-dimensional cell cultures in drug discovery and development. *SLAS Discov.* 22(5), 456–472 (2017).

•• **Use of 3D cell cultures instead of 2D simulated the tumor microenvironment much better.**

2. Cheng HW, Chen YF, Wong JM *et al.* Cancer cells increase endothelial cell tube formation and survival by activating the PI3K/Akt signalling pathway. *J. Exp. Clin. Cancer Res.* 36(1), 27 (2017).
3. Laidler P, Dulinska J, Lekka M, Lekki J. Expression of prostate specific membrane antigen in androgen-independent prostate cancer cell line PC-3. *Arch. Biochem. Biophys.* 435(1), 1–14 (2005).
4. Mellman DL, Gonzales ML, Song C *et al.* A PtdIns4, 5P2-regulated nuclear poly(A) polymerase controls expression of select mRNAs. *Nature* 451(7181), 1013–1017 (2008).
5. Yu C, Gong Y, Zhou H *et al.* Star-PAP, a poly(A) polymerase, functions as a tumor suppressor in an orthotopic human breast cancer model. *Cell Death Dis.* 8(2), e2582 (2017).
6. Chao WT, Daquinag AC, Ashcroft F, Kunz J. Type I PIPK-alpha regulates directed cell migration by modulating Rac1 plasma membrane targeting and activation. *J. Cell Biol.* 190(2), 247–262 (2010).
7. Xie Z, Chang SM, Pennypacker SD, Liao EY, Bikle DD. Phosphatidylinositol-4-phosphate 5-kinase 1alpha mediates extracellular calcium-induced keratinocyte differentiation. *Mol. Biol. Cell* 20(6), 1695–1704 (2009).
8. Semenas J, Hedblom A, Miftakhova RR *et al.* The role of PI3K/AKT-related PIP5K1alpha and the discovery of its selective inhibitor for treatment of advanced prostate cancer. *Proc. Natl Acad. Sci. U S A* 111(35), e3689–e3698 (2014).
9. Flemming A. Cancer: lipid kinase PIP5K1alpha as a new target in prostate cancer. *Nat. Rev. Drug Discov.* 13(10), 723 (2014).

•• **Target has already been established, but there are no data to date to support its role in lymph node metastasis.**

10. Bosse F, Hasse B, Pippirs U, Greiner-Petter R, Muller HW. Proteolipid plasmolipin: localization in polarized cells, regulated expression and lipid raft association in CNS and PNS myelin. *J. Neurochem.* 86(2), 508–518 (2003).
11. Aranda JF, Reglero-Real N, Kremer L *et al. MYADM* regulates Rac1 targeting to ordered membranes required for cell spreading and migration. *Mol. Biol. Cell* 22(8), 1252–1262 (2011).

- **Role of *MYADM* in metastasis is supported by new 3D experiments.**

12. Ridley AJ, Schwartz MA, Burridge K *et al.* Cell migration: integrating signals from front to back. *Science* 302(5651), 1704–1709 (2003).
13. Fehon RG, Mcclatchey AI, Bretscher A. Organizing the cell cortex: the role of ERM proteins. *Nat. Rev. Mol. Cell Biol.* 11(4), 276–287 (2010).
14. Clark PR, Manes TD, Pober JS, Kluger MS. Increased ICAM-1 expression causes endothelial cell leakiness, cytoskeletal reorganization and junctional alterations. *J. Invest. Dermatol.* 127(4), 762–774 (2007).
15. Aranda JF, Reglero-Real N, Marcos-Ramiro B *et al. MYADM* controls endothelial barrier function through ERM-dependent regulation of *ICAM-1* expression. *Mol. Biol. Cell* 24(4), 483–494 (2013).
16. Kwiatkowska K. One lipid, multiple functions: how various pools of PI(4,5)P(2) are created in the plasma membrane. *Cell. Mol. Life Sci.* 67(23), 3927–3946 (2010).
17. Heissler SM, Sellers JR. Kinetic adaptations of myosins for their diverse cellular functions. *Traffic* 17(8), 839–859 (2016).
18. Makowska KA, Hughes RE, White KJ, Wells CM, Peckham M. Specific myosins control actin organization, cell morphology, and migration in prostate cancer cells. *Cell Rep.* 13(10), 2118–2125 (2015).

- ***MYO1B* is associated with migration in prostate cancer; this is also supported by the 3D cultures used in the authors' experiments.**

19. Zhang HR, Lai SY, Huang LJ *et al. Myosin 1b* promotes cell proliferation, migration, and invasion in cervical cancer. *Gynecol. Oncol.* 149(1), 188–197 (2018).
20. Ohmura G, Tsujikawa T, Yaguchi T *et al.* Aberrant *myosin 1b* expression promotes cell migration and lymph node metastasis of HNSCC. *Mol. Cancer Res.* 13(4), 721–731 (2015).
21. Yamada A, Mamane A, Lee-Tin-Wah J *et al.* Catch-bond behaviour facilitates membrane tubulation by non-processive *myosin 1b*. *Nat. Commun.* 5, 3624 (2014).
22. Diz-Munoz A, Krieg M, Bergert M *et al.* Control of directed cell migration *in vivo* by membrane-to-cortex attachment. *PLoS Biol.* 8(11), e1000544 (2010).
23. Almeida CG, Yamada A, Tenza D, Louvard D, Raposo G, Coudrier E. *Myosin 1b* promotes the formation of post-Golgi carriers by regulating actin assembly and membrane remodelling at the trans-Golgi network. *Nat. Cell Biol.* 13(7), 779–789 (2011).
24. Komaba S, Coluccio LM. Localization of *myosin 1b* to actin protrusions requires phosphoinositide binding. *J. Biol. Chem.* 285(36), 27686–27693 (2010).
25. De Marzo AM, Bradshaw C, Sauvageot J, Epstein JI, Miller GJ. CD44 and CD44v6 downregulation in clinical prostatic carcinoma: relation to Gleason grade and cytoarchitecture. *Prostate* 34(3), 162–168 (1998).
26. Omara-Opyene AL, Qiu J, Shah GV, Iczkowski KA. Prostate cancer invasion is influenced more by expression of a CD44 isoform including variant 9 than by Muc18. *Lab. Invest.* 84(7), 894–907 (2004).
27. Jiang Y, Dai J, Yao Z, Shelley G, Keller ET. Abituzumab targeting of alphaV-class integrins inhibits prostate cancer progression. *Mol. Cancer Res.* 15(7), 875–883 (2017).
28. Van Der Horst G, Van Den Hoogen C, Buijs JT *et al.* Targeting of alpha(v)-integrins in stem/progenitor cells and supportive microenvironment impairs bone metastasis in human prostate cancer. *Neoplasia* 13(6), 516–525 (2011).
29. Gajula RP, Chettiar ST, Williams RD *et al.* The twist box domain is required for Twist1-induced prostate cancer metastasis. *Mol. Cancer Res.* 11(11), 1387–1400 (2013).
30. Wei J, Xu G, Wu M *et al.* Overexpression of vimentin contributes to prostate cancer invasion and metastasis via src regulation. *Anticancer Res.* 28(1A), 327–334 (2008).
31. Zhao Y, Yan Q, Long X, Chen X, Wang Y. Vimentin affects the mobility and invasiveness of prostate cancer cells. *Cell Biochem. Funct.* 26(5), 571–577 (2008).
32. Voeller HJ, Truica CI, Gelmann EP. Beta-catenin mutations in human prostate cancer. *Cancer Res.* 58(12), 2520–2523 (1998).
33. Francis JC, Thomsen MK, Taketo MM, Swain A. Beta-catenin is required for prostate development and cooperates with Pten loss to drive invasive carcinoma. *PLoS Genet.* 9(1), e1003180 (2013).
34. Myklebust MP, Fluge O, Immervoll H *et al.* Expression of *DSG1* and *DSC1* are prognostic markers in anal carcinoma patients. *Br. J. Cancer* 106(4), 756–762 (2012).
35. Pellinen T, Blom S, Sanchez S *et al. ITGB1*-dependent upregulation of *Caveolin-1* switches TGFbeta signalling from tumour-suppressive to oncogenic in prostate cancer. *Sci. Rep.* 8(1), 2338 (2018).
36. Heidegger I, Kern J, Ofer P, Klocker H, Massoner P. Oncogenic functions of *IGF1R* and *INSR* in prostate cancer include enhanced tumor growth, cell migration and angiogenesis. *Oncotarget* 5(9), 2723–2735 (2014).
37. D'amico AV, Whittington R, Kaplan I *et al.* Calculated prostate carcinoma volume: the optimal predictor of 3-year prostate specific antigen (PSA) failure free survival after surgery or radiation therapy of patients with pretreatment PSA levels of 4–20 nanograms per milliliter. *Cancer* 82(2), 334–341 (1998).

38. Preisser F, Van Den Bergh RCN, Gandaglia G *et al.* Effect of extended pelvic lymph node dissection on oncologic outcomes in patients with D'Amico intermediate and high risk prostate cancer treated with radical prostatectomy: a multi-institutional study. *J. Urol.* 203(2), 338–343 (2020).

39. Gabriele D, Jereczek-Fossa BA, Krengli M *et al.* Beyond D'Amico risk classes for predicting recurrence after external beam radiotherapy for prostate cancer: the Candiolo classifier. *Radiat. Oncol.* 11, 23 (2016).

40. Mazzone E, Preisser F, Nazzani S *et al.* The effect of lymph node dissection in metastatic prostate cancer patients treated with radical prostatectomy: a contemporary analysis of survival and early postoperative outcomes. *Eur. Urol. Oncol.* 2(5), 541–548 (2019).

41. Muteganya R, Goldman S, Aoun F, Roumeguere T, Albisinni S. Current imaging techniques for lymph node staging in prostate cancer: a review. *Front. Surg.* 5, 74 (2018).